ELSEVIER

Biophysical Chemistry 101–102 (2002) 187–201

Biophysical Chemistry

www.elsevier.com/locate/bpc

Evidence of turn and salt bridge contributions to β-hairpin stability: MD simulations of C-terminal fragment from the B1 domain of protein G

Jerry Tsai[a,*], Michael Levitt[b]

[a]*Department of Biochemistry and Biophysics, 2128 Texas A&M University, College Station, TX 77843-2128, USA*
[b]*Department of Structural Biology, Fairchild Building D109, Stanford University, Stanford, CA 94305-5400, USA*

Received 23 January 2002; received in revised form 18 April 2002; accepted 18 April 2002

Abstract

We ran and analyzed a total of eighteen, 10 ns molecular dynamics simulations of two C-terminal β-hairpins from the B1 domain of Protein G: twelve runs for the last 16 residues and six runs for the last 15 residues, G41–E56 and E42–E56, respectively. Based on their CαRMS deviation from the starting structure and the pattern of stabilizing interactions (hydrogen bonds, hydrophobic contacts, and salt bridges), we were able to classify the twelve runs on G41–E56 into one of three general states of the β-hairpin ensemble: 'Stable', 'Unstable', and 'Unfolded'. Comparing the specific interactions between these states, we find that on average the stable β-hairpin buries 287 Å^2 of hydrophobic surface area, makes 13 hydrogen bonds, and forms 3 salt-bridges. We find that the hydrophobic core prefers to make some specific contacts; however, this core does not require optimal packing. Side-chain hydrogen bonds stabilize the β-hairpin turn with strong stabilizing interactions primarily due to the carboxyl of D46 with contributions from T49 hydroxyl. Buoyed by the strength of the hydrophobic core, other hydrogen bonds, primarily main-chain, guide the β-hairpin into registration by forming a loose network of interactions, making an approximately constant number of hydrogen bonds from a pool of possible candidates. In simulations on E42–E56, where the salt bridge closing the termini is not favored, we observe that all the simulations show no 'Stable' behavior, but are 'Unstable' or 'Unfolded'. We can estimate that the salt-bridge between the termini provides approximately 1.3 kcal/mol. Altogether, the results suggest that the β-hairpin folds beginning at the turn, followed by hydrophobic collapse, and then hydrogen bond formation. Salt bridges help to stabilize the folded conformations by inhibiting unfolded states.

Keywords: β-hairpin stability; Protein interactions; Hydrogen bonds; Hydrophobic interactions; Salt bridges; Molecular dynamics simulation

*Corresponding author. Tel.: +01-979-458-3377; fax: +01-979-845-9274.
E-mail address: JerryTsai@TAMU.edu (J. Tsai).

0301-4622/02/$ - see front matter
PII: S0301-4622(02)00198-9

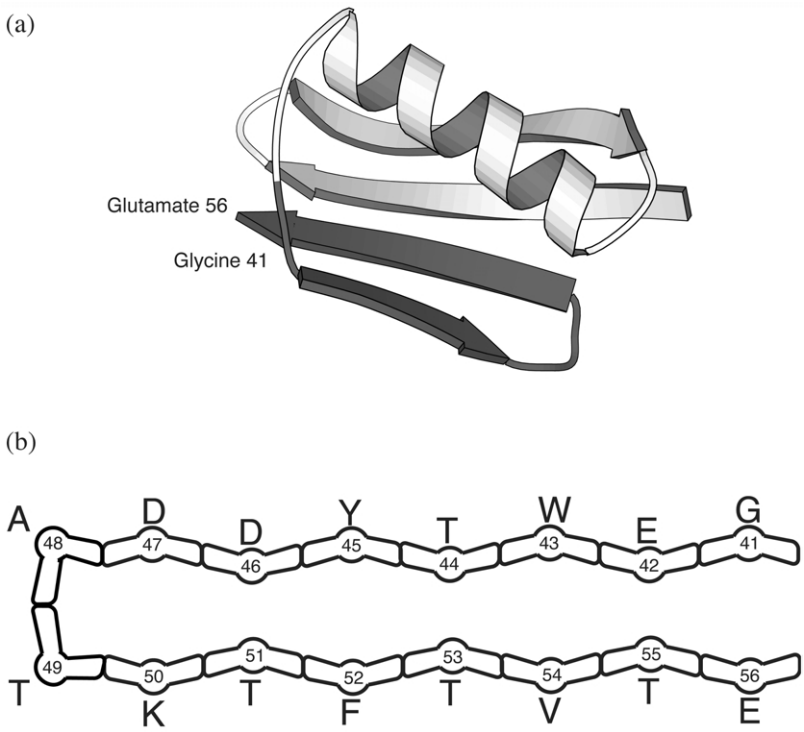

Fig. 1. Origin and schematic of the β-hairpin. (a) The complete structure of the B1 domain of Protein G is shown using the 1PGB structure file [47]. The figure was made using the programs RASMOL [50] for orientation and MOLSCRIPT [51] for output. Residues G41 to E56 are highlighted in a darker shade of gray. (b) A schematic of the excised β-hairpin. The kinks represent which side (hydrophobic or hydrophilic) of the hairpin a residue is pointing (explained in the text). The residues pointing out are on 'hydrophobic side' of the hairpin, while those pointing in are on the 'hydrophilic side'.

1. Introduction

While two forms of local protein structure had been predicted a number of years earlier [1,2], a proper appreciation of protein primary and secondary structure did not enter the literature until later when it was discussed by Linderstrøm–Lang and Schellman [3]. While John Schellman performed much of his work in proteins on the thermodynamics of folding [4–8], he still published some work studying the formation of α-helices [9,10]. Such investigations into secondary structure formation provide simple systems to study the basic units of protein structure. As Schellman's and others' work indicates [9,11,12], more has been done with α-helices over β-sheets due to the inherent stability of helices in solution.

Work on even the simplest β-sheet, the two-stranded β-hairpin, has been limited by their low stability and/or tendency to aggregate in solution. In the past decade, stable hairpins and sheets have been characterized experimentally [13–21]. These results have provided tractable systems for comparison with molecular dynamics simulations, although simulations of β-sheets had been done previously by a number of groups [22–30]. Of the experimental systems, many groups have chosen to characterize the C-terminal, 16 residue β-hairpin from the B1 domain of Protein G (Fig. 1). Its intrinsic stability was first proposed by Kobayashi, et al. [20], and studied in detail [14,15,17,19,21]. In agreement with experimental results but differing with the zippering theory of hairpin folding

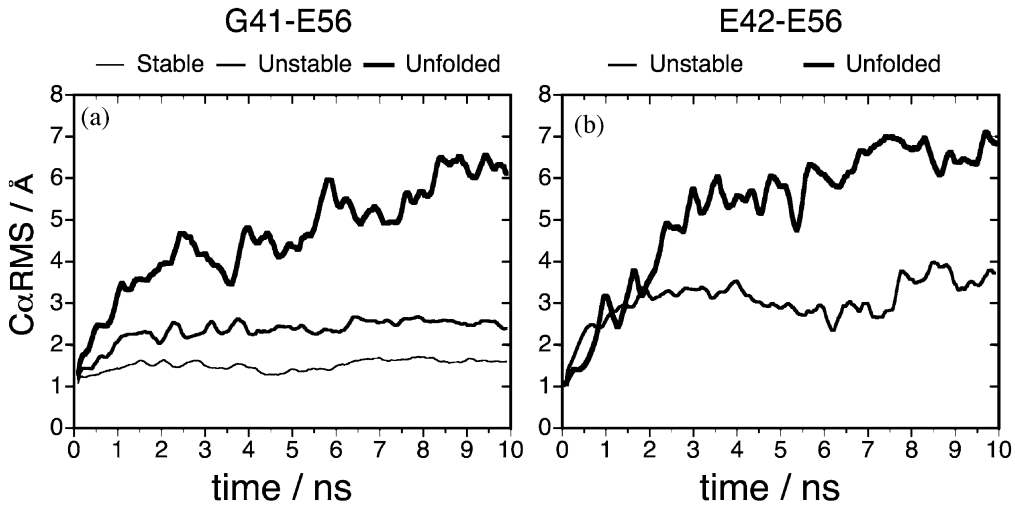

Fig. 2. CαRMS vs. Time. To filter out noise, we smoothed the curves by averaging over a window of 50 values. (a). The curves for the three states found in the G41–E56 simulations. For clarity, we did not add error bars; however, we list the standard deviation between runs as follows: the 7 'Stable' simulations were 0.277 Å; the three 'Unstable' simulations were 0.899 Å; and the two 'Unfolded' simulations were 1.254 Å. (b). The curves for the two states observed from the simulations of the E42–E56 β-hairpin. Standard deviations between the runs for the 'Unstable' and 'Unfolded' states are 0.582 and 0.657 Å, respectively.

[17], these simulations have identified that the hydrophobic core provides most of the hairpin's stability [29–37] and seems to be the nucleation site for folding [33,34,36]. The backbone hydrogen bonds seem to only play a crucial role in the latter stages of folding [35,36], although some recent theoretical work suggests that the hydrogen bonds form concomitantly with the hydrophobic core [30]. Another recent theoretical paper on this hairpin has found evidence of a helical intermediate not seen elsewhere [29]. There is some disagreement as to the role of the hairpin turn in the folding pathway [31,32,35,36,38], and there is no discussion of salt bridge contributions. In this paper, we address these issues of the turn and salt bridges in the stability of a β-hairpin in a description of a very extensive series of molecular dynamics simulations of the standard 16-residue β-hairpin and a shorter 15-residue β-hairpin from the B1 domain of Protein G.

Molecular dynamics simulations of proteins in solution provide a detailed view of molecular interactions not normally seen in experiment. In doing so, however, simulations suffer from the inaccuracy of the energy functions and the lack of sufficient sampling. The reason for both of these limitations is that computer resources necessarily limit molecular dynamics simulations. Here we use a particularly efficient empirical potential energy calculation [39] to speed up calculations enough to run several long trajectories that give adequate sampling. Of course, the accuracy of calculations using any empirical force field is prima facie suspect: molecular dynamics should generally be done on systems allowing comparison with experiment. For the β-hairpin structure studied in this paper, as with previous simulation studies, we can compare our data with the large body of experimental and theoretical work done on the hairpin as well as the complete domain. Each dynamics trajectory only follows the progression in time of one protein molecule, whereas experimental results generally measure the average over an ensemble of many, many molecules. To offset this shortcoming, we ran a total of 18 different trajectories for two β-hairpins, each lasting 10 nanoseconds (ns). Although each simulation follows the time-course of a single molecule, certain trajectories exhibited similar behavior in their backbone fluctuations and pattern of protein interactions (including salt bridg-

es). Using this information, we are able to identify different states of the hairpin ensemble. From the results provided by these simulations, we propose a role for the salt bridges in protein stability and also clarify the turn's role in the folding pathway of the β-hairpin.

To simplify our discussion of interactions, we will use a shorthand notation that incorporates the amino acids one letter code, its residue number, and atom group (if necessary). For example, we will use W43..F52 to represent the hydrophobic contact between tryptophan 43 and phenylalanine 52. For hydrogen bonds and salt bridges, we will add the atom groups involved to indicate direction. An example of a hydrogen bond is T44_H..F52_O between threonine 44's main-chain amino hydrogen and phenylalanine 52's main-chain carbonyl oxygen. An example of a salt bridge is D47_OD..K50_NZ between aspartate 47's side-chain carboxyl group and lysine 50's side-chain amino group.

2. Results/analysis

We ran twelve simulations on the β-hairpin using the last 16 residues of the B1 domain of protein G (Fig. 1). Runs using this peptide will be denoted G41–E56. We also ran six more simulations to test a salt bridge's contribution to β-hairpin stability. The peptide used in these was one residue shorter and spanned the last 15 residues of the protein G, B1 domain (see bottom of Fig. 1). Runs with this 15 mer will be designated by E42–E56. All simulations were run for 10 ns. Although each of the trajectories on the same peptide is equivalent to another, the use of different initial random number seeds gives rise to a total of eighteen independent samplings of hairpin behavior at room temperature. Our analysis of these hairpin simulations consisted of the root mean deviation of the α carbons (CαRMS) of the simulation structure from the starting structure (see Fig. 2). We also evaluated the β-hairpin for three types of protein interactions: hydrogen bonds (HB), hydrophobic contacts (HC), and salt bridges (SB). Table 1 summarizes the percent occupancy of these three types of protein interactions found in simulations of the β-hairpin as well as the CαRMS deviation averaged over a certain group of runs (see below). To identify which residues were contributing to β-hairpin stability, we further separated the types of protein interactions into their individual pairs as listed in Table 2 and presented in Fig. 3. The list consists of all the native interactions as well as those existing for more than half the time (more than 50% occupancy). We separate the list based on where the interactions occur. For reference, Fig. 3 illustrates Table 2's list of interactions in a corresponding fashion, in order to provide a sense of the physical location of an interaction or set of interactions. The table and figure splits the interactions into three types based on their location on the hairpin. One side of the hairpin possesses predominantly hydrophobic residues and as such, is named the 'hydrophobic side'. The hydrogen bonding interactions by main-chain carbonyl and amino nitrogen atoms are named 'in plane', although the β-hairpin is not flat as depicted by Fig. 1. The side opposite to the hydrophobic side contains all hydrophilic residues and so is named the 'hydrophilic side'. Also, in our discussion, we make a distinction between those interactions occurring across the β-hairpin, between strands as 'interstrand' and those occurring within a strand as 'intrastrand'.Figs. 4 and 5

2.1. G41–E56 β-hairpin

Based on an individual run's CαRMS from the starting structure, the twelve simulations of the G41–E56 β-hairpin could be categorized into three groups: 'Stable', 'Unstable', and 'Unfolded'. Fig. 2a graphs the mean CαRMS curve vs. simulation time for each of the three types, where the CαRMS is averaged over the runs of each type. The runs were grouped as follows: 7 'Stable' simulations exhibited a CαRMS that remained below 2 Å during the entire run; 3 'Unstable' simulations exhibited CαRMS values that oscillated between 2 to 4 Å; 2 'Unfolded' simulations exhibited a CαRMS curve with a great deal of variability and peak values above 7 Å. Using these general groupings as a guide, we will describe the protein interactions that stabilize these three states.

Table I. Average Protein Interactions

In the first column for comparison, we show the values for the native β-hairpin. For each grouping of simulations, the number of simulations in that group is listed. <CαRMS Deviation> in Å refers to the average deviation of the CαRMS within runs, as opposed to between runs in a group which was reported in the legend to Figure 2. This value measures how much the structure deviated over the length of the simulation. For hydrophobic contacts, the values are in Å^2, and we split these interactions in the following manner. Main to main refers to hydrophobic interactions between mainchain atoms. Main to side is mainchain to sidechain atoms, and side to side are sidechain, hydrophobic interactions. The description finishes up with hydrogen bonds and salt bridges. (A) This table shows the averages based on the initial groupings by CαRMS. (B) This table shows the averages for subgroups: the "A", "B", and "C" subgroups of the "Stable" G41-E56 β-hairpin and the two subgroups of the "Unstable" E42-E56 β-hairpin.

										G41-E56								E42-G42					
		Interaction								Stable A		Stable B		Stable C		Unstable		Unfolded		Unstable A		Unstable B		Unfolded	
#	TP	Res/Atom			n/-	Res/Atom				%	SA	%	SA	%	SA	%	SA	%	SA	%	SA	%	SA	%	SA
		Hydrophobic Side																							
a	SB	G	41	NT	-	E	56	OXT		36		99		-		46		-		- *		11*		<1*	
b	SB	G	41	NT	-	E	56	OE		21		-		75		73		<1		- *		- *		- *	
c	HB	E	42	H	-	E	56	OE		-		14		47		33		-		-		-		-	
d	HC	W	43		n	V	54			93	7	84	13	90	9	77	12	36	10	16	12	45	11	16	14
e	HC	W	43		n	F	52			100	20	94	14	98	20	61	17	28	14	87	13	26	10	19	13
f	HC	Y	45		n	F	52			89	14	92	17	96	17	49	14	29	11	100	17	24	11	72	13
g	HC	Y	45		-	K	50			84	9	78	4	94	5	59	4	23	6	97	5	61	5	45	5
h	HC	D	47		-	K	50			46	2	44	1	67	2	45	2	29	2	31	2	52	2	62	1
i	SB	D	47	OD	-	K	50	NZ		90		100		100		100		100		41		100		99	
j	HC	V	54		-	E	56			40	5	12	2	85	6	40	4	19	2	14	3	11	2	16	3
k	HC	F	52		-	V	54			65	7	70	9	64	5	46	8	73	10	80	8	45	8	57	9
l	HC	W	43		-	Y	45			98	13	71	11	85	9	56	8	48	11	94	15	73	10	69	12
m	HC	K	50		-	F	52			57	6	42	5	65	4	34	6	53	9	57	9	40	10	70	9
n	HC	Y	45		n	D	47			85	5	90	6	97	5	92	7	56	5	100	6	57	5	91	7
o	HB	Y	45	HH	n	D	47	OD		55		59		96		60		13		80		21		42	
		In plane of Hairpin																							
a	HB	G	41	O	-	E	56	H		20		-		47		20		-		- *		- *		- *	
b	HB	G	41	O	-	T	55	H		17		<1		43		<1		-		- *		- *		- *	
c	HB	E	42	H	n	T	55	O		2		1		<1		<1		<1		<1		<1		<1	
d	HB	E	42	O	n	T	55	H		88		14		37		<1		<1		<1		<1		<1	
e	HB	W	43	O	-	V	54	H		-		46		-		-		-		-		-		-	
f	HB	T	44	H	n	T	53	O		70		21		60		31		7		2		3		5	
g	HB	T	44	O	n	T	53	H		1		62		4		16		3		2		5		4	
h	HB	T	44	H	-	F	52	O		81		-		57		5		-		-		-		-	
i	HB	Y	45	H	-	F	52	O		65		-		61		13		-		-		-		-	
j	HB	Y	45	H	-	T	51	O		24		<1		<1		<1		<1		-		-		-	
k	HB	D	46	H	n	T	51	O		63		65		88		36		11		85		5		15	
l	HB	D	46	O	n	T	51	H		40		57		89		30		12		93		16		21	
m	HB	D	46	O	-	K	50	H		45		90		51		60		15		43		58		42	
n	HB	D	46	O	n	T	49	H		2		4		6		3		1		3		4		2	
		Hydrophillic Side																							
a	HB	E	42	O	-	T	55	HG1		88		8		46		<1		<1		<1		<1		<1	
b	HC	E	42		n	T	55			50	3	4	2	37	3	5	3	1	2	2	4	1	3	<1	2
d	HC	T	44		-	T	55			53	2	12	4	19	2	22	3	3	4	15	5	2	2	24	6
d	HC	T	44		-	T	53			76	4	37	6	50	4	41	6	14	3	4	0	8	5	16	5
e	HB	D	46	OD	-	T	51	HG1		61		4		2		34		83		-		26		63	
f	HC	D	46		n	T	51			29	3	31	3	17	4	24	3	44	2	22	4	20	2	57	3
g	HB	D	46	OD	-	T	51	H		59		4		2		34		82		-		25		57	
h	HB	D	46	OD	-	K	50	H		62		14		3		38		36		-		22		58	
i	HB	D	46	OD	-	T	49	HG1		80		67		6		66		35		-		11		57	
j	HC	D	46		n	T	49			38	<1	57	1	24	1	26	1	18	<1	14	1	43	1	75	1
k	HB	D	46	OD	-	T	49	H		80		67		6		66		36		-		57		91	
l	SB	G	41	NT	-	E	42	OE		57		68		-		-		88		<1*		17*		35*	
m	HC	T	53		-	T	55			39	3	63	6	21	4	52	6	13	3	90	6	18	3	16	5
n	HC	E	42		-	T	44			5	3	20	3	11	3	23	3	3	3	1	1	27	3	10	2
o	HC	D	46		n	A	48			56	2	56	1	63	2	58	1	28	1	59	1	61	2	41	1
p	HB	D	46	OD	n	A	48	H		59		56		5		38		16		<1		27		32	
q	HC	T	49		-	T	51			52	6	66	6	66	7	53	6	30	5	64	6	80	7	46	8
r	HC	A	48		n	T	49			31	2	9	2	35	3	29	2	42	2	52	3	27	2	9	2

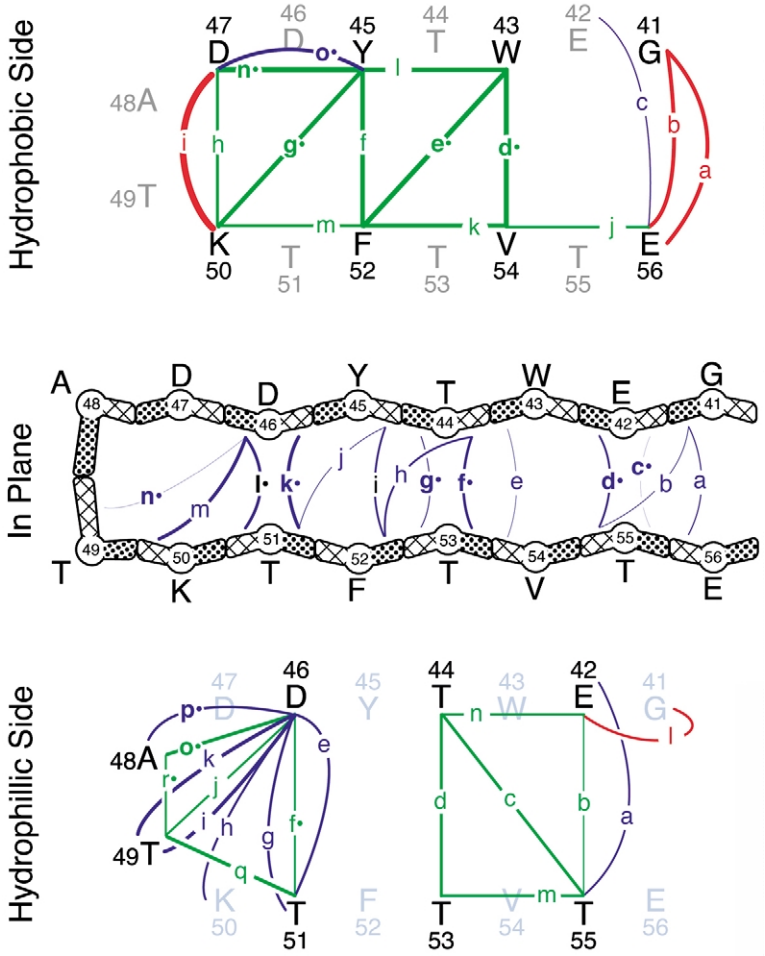

Fig. 3. Schematic of β-hairpin Interactions. Interactions are colored and categorized to correspond with those in Table 1. For further clarity, curved lines represent hydrogen bonds and salt bridges, while straight ones are hydrophobic contacts. Hydrogen bonds are blue, salt bridges are red, and side-chain hydrophobic contacts are green. Letters are ordered beginning from the open termini to the turn, and correspond to those in Table 2. Interactions are grouped according to one of three locations on the hairpin: the hydrophobic side, in plane, and hydrophilic side. Within each location, interactions occurring across the β-hairpin (interstrand) are listed first and those within a strand (intrastrand) are listed second. Interactions found in the starting 'native' structure are marked with a '●' next to their letter. Thickness of lines relates directly to percent occupancy during an average all 'Stable' simulations from the G41–E56 β-hairpin (see Table 2). For the two sides of the hairpin, residues belonging to each respective side are displayed in black text and represent the side-chain using the amino acid's single letter code and residue number (according to the full length B1 domain of Protein G). For hydrogen bonds and salt bridges, interactions of side-chain to side-chain connect the sides facing in on the hairpin and those between side-chain and main-chain connect a side facing in to the either the carbonyl or amide side of the residue. The residues in gray should have no interactions on that side in a properly formed β-sheet. This breaks down for certain residues like those near the termini (i.e. interaction 'l' on the hydrophilic side: the salt bridge G41_NT..E42_OE) and particularly for the hydrogen bonds made by D46 near the turn (i.e. the hydrogen bond D46_OD..K50_NZ). For the 'in plane' representation, the main-chain is shown. Each amino acid is represented by the following: hatched side for amide group, circled number below the single letter code for the side-chain, and polka dots for the carbonyl group. Like the similar representation in Fig. 1B, direction of the kink refers to which side of the β-hairpin the residue begins on: the residues pointing out are on 'hydrophobic side' of the hairpin, while those pointing in are on the 'hydrophilic side'. The hatches and polka dots are 'in plane'.

Table II. Interactions

Protein interactions are described and correspond to those shown in Figure 3. The letter under the "#" identifies the interaction with those of the same location and letter displayed in Figure 3. "TP" refers to the type of interaction: SB - salt bridge (red), HB - hydrogen bond (blue), HC – sidechain hydrophobic contact (green). Entries are colored to match the interactions colors in Figure 3. "Res/Atom" describes which residues (HC) or atoms (HB and SB) are involved in the interaction pair. A "n/-" indicates whether or not the interaction is found in the native crystal structure: "n" for native and "-" for not. "%" is the average percent occupancy for simulations of that ensemble state and a "-" indicates the interaction was not found in those simulations. For HC interactions, SA refers to the average buried surface area due to the interaction (in Å^2). Interactions are split up depending on their location on the sheet. Ordering corresponds to an interaction's proximity along the G41-E56 β-hairpin starting from the open free termini to the turn (see Figure 3). For the E42-E56 β-hairpin, the N-terminal (NT) amino group is on the E42 residue (since there is no G41 in this structure). A "*" marks where this is the case, and the interaction should be considered from the E42 N-terminus.

Interactions		Native	G41-E56			E42-E56	
			Stable	Unstable	Unfolded	Unstable	Unfolded
Number of Runs		na	7	3	2	4	2
<CαRMS Deviation> / Å		na	0.24	0.47	1.57	0.63	1.63
Hydrophobic Contacts	main to main	36	52	41	38	37	38
	side to main	44	55	51	33	44	39
	side to side	118	182	152	142	154	150
	Total	198	287	247	213	234	226
Hydrogen Bonds		9	13	11	7	5	8
Salt Bridges		0	3	2	2	1	2

A

Interactions		Native	G41-E56 Stable			E42-E56 Unstable	
			Stable A	Stable B	Stable C	Unstable A	Unstable B
Number of Runs		na	3	2	2	1	3
<CαRMS Deviation> / Å		na	0.20	0.32	0.14	0.68	0.61
Hydrophobic Contacts	main to main	36	53	50	47	37	36
	side to main	44	55	48	61	46	43
	side to side	118	190	171	182	189	143
	Total	198	298	269	289	272	222
Hydrogen Bonds		9	15	12	11	4	6
Salt Bridges		0	2	3	2	<1	1

B

2.2. *Stable*

On average, the 7 simulations exhibiting 'Stable' β-hairpin behavior bury 287 Å^2 of hydrophobic surface area; form 13 hydrogen bonds; and make 2 salt bridges (Table 1A). Looking at the schematic of interactions in Fig. 3, we find the strong non-polar core on the hydrophobic side of the β-hairpin. On the hydrophilic side, we see the numerous interactions made by D46 and few high occupancy interactions in the middle of the β-hairpin. The CαRMS is a coarse measure of similarity, since different conformations can have

the same CαRMS. Therefore, we decided to investigate the individual protein interaction pairs that contribute to the β-hairpin's stability. Such an analysis reveals some remarkable differences between these 'Stable' runs and allows us to further classify the 7 'Stable' simulations into three more groups: 'A', 'B' and 'C'.

The first group 'Stable A' represents 3 simulations with a consistent hydrophobic core that buries on average 298 Å^2 of non-polar surface area, which is more than any other set of simulations (Table 1B). This core is centered on the interaction between W43 and F52, which occurs 100% of the time in all three simulations. Of all the hydrophobic interactions, this W43..F52 one buries the most surface area (20 Å^2 on average) and connects the two strands in the middle of the β-hairpin. On the opposite side of the β-hairpin, the hydrophobic interactions are largely lost during the simulation. On average, these simulations form 15 hydrogen bonds, the most of any simulation. The hydrogen bonding pattern does not preserve the native β-hairpin pattern, but indicates a β-bulge occurs at the 'in plane', main-chain hydrogen bond between T44_H..F52_O. Other significant hydrogen bonds occur on the hydrophilic side. The E42_OE..T55_HG1 hydrogen bond closes the termini, while D46_OD makes numerous and steady hydrogen bonds across the turn. While on average there are 2 salt bridges, the only significant salt bridge occurs at D47_OD..K50_NZ. The other one is split between closing the termini and a non-stabilizing, intrastrand salt bridge G41_NT..E42_OE.

The second group, 'Stable B', represents 2 simulations with a somewhat looser hydrophobic core that buries on average 269 Å^2 of non-polar surface area mostly on the hydrophobic side of the β-hairpin. The core is less centralized but retains many native hydrophobic interactions across the β-hairpin made at over 80% frequency: W43..V54, W43..F52, Y45..F52 and Y45..D47. The average number of hydrogen bonds made is 13. D46 still makes many side-chain hydrogen bonds across the turn, but we find that many of the native main-chain hydrogen bonds in the plane of the β-hairpin and towards the termini exhibit decreased frequencies. In contrast, the salt bridges which stabilize the termini (between G41's teminal amino group and E56's carboxyls: G41_NT..E56_OE and G41_NT..E56_OXT) and the hairpin turn (D47_OD..K50_NZ) show very high occupancies of 99 and 100%, respectively. The local, non-stabilizing G41_NT..E42_OE salt bridge is also made often, so that there are on average 3 salt bridges in this group of simulations.

The third group, 'Stable C', represents 2 simulations that were immediately recognizable as similar from their CαRMS curves (data not shown). As can be seen from the average standard deviations within runs in Table 1, this group of simulations shows the lowest mean CαRMS deviation of 0.14 Å. Such a low value suggests that the β-hairpin's structure fluctuates very little and is in rigid state. Viewing these 2 simulations, we find that early in simulation the side-chain of residue W43 flips. This group of simulations then buries 298 Å^2 of non-polar surface area primarily on the hydrophobic side of the β-hairpin. The interactions are almost all above 80% occupancy up and down the hairpin. Therefore, the flipping of the W43 residue must allow more consistent packing across the β-hairpin. This 'C' group possesses an average of 11 hydrogen bonds, which is the fewest number made by any of the 'Stable' simulations. This is primarily due to the lack of D46_OD hydrogen bonding across the turn. However, this group makes more constant, native hydrogen bonds in the plane of the β-hairpin by main-chain atoms. Also, the relaxation caused by the flipping of the W43 may allow for the high occupancy of the hydrogen bond Y45_HH..D47_OD. This helps tie the hydrophobic core into the salt bridge that is made 100% of time across the β-hairpin turn by D47_OD..K50_NZ. With an average of 2 salt bridges, the runs make their other salt bridge across the termini at only G41_NT..E56_OE.

2.3. Unstable

On average, the 3 simulations exhibiting 'Unstable' β-hairpin behavior bury 40 Å^2 less hydrophobic surface area (average of 247 Å^2). This drop is due to a reduction in all hydrophobic interactions across the β-hairpin. Higher occupancy interactions occur within a strand between neighbors like

the one from Y45..D47. One long-range hydrophobic interaction of note is W43..V54, near the chain termini. We also find that the average number of hydrogen bonds is lower than for the 'Stable' runs at 11. As can be seen in Table 2, all main-chain hydrogens bonds in the plane of the β-hairpin are lost. In contrast, hydrogen bonds made by the D46_OD remain high in occupancy. The two salt bridges made in these simulations are the one bridging the turn by D47_OD..K50_NZ (made 100% of the time) and the other split between the two possibilities for G41_NT to either of E56's carboxyls: E56_OE or E56_OXT. Of these two at the termini, the salt bridge G41_NT..E56_OE is preferred (75% occupancy) over G41_NT..E56_OXT (46% occupancy). These results suggest that the β-hairpin has opened in the middle and is closed by the turn interactions on one end and the W43..V54 hydrophobic contact in concert with the G41_NT salt bridges on the other. Visual inspection confirmed that this was the state of the β-hairpin in the 'Unstable' G41–E56 group.

2.4. Unfolded

On average, the two simulations exhibiting 'Unstable' β-hairpin behavior bury on average of just 213 $Å^2$ of hydrophobic surface area. The β structure denatures rapidly, as exhibited by the immediate increase in the CαRMS to the starting structure (Fig. 2) and viewing of the trajectories. In this group of simulations, there is no hydrophobic interaction across the β-hairpin that is made over 40% of the time. Again, the high occupancy interactions occur between neighboring resides within a strand. Only 7 hydrogens bonds are made on average. All the main-chain, in plane hydrogen bonds display occupancies that suggest they are not formed for the majority of the simulations. High frequency hydrogen bonds are predominantly made by D46_OD (see Table 2). For instance, the most persistent hydrogen bonds occur at D46_OD..T51_HG1. The high occupancy of this non-native hydrogen bond suggests that the turn has a certain amount of structure. Two salt bridges are made on average: the one across the turn D47_OD..K50_NZ and the other intrastrand G41_NT..E42_OE. The protein interactions in this group of simulations describe a β-hairpin that has effectively opened up with only the turn retaining some structure.

2.5. E42–E56 β-hairpin

The previous set of simulations indicated a role for terminal salt bridges in the stability of the hairpin. To test this stability, we ran six more simulations, but with a β-hairpin shortened by one residue. The E42–E56 β-hairpin begins with the termini out of register by one residue, so therefore, doesn't favor salt bridge formation at the termini. The CαRMS curves exhibited less stable behavior than with the longer β-hairpin. Again, we could loosely group the simulations into sets based on their CαRMS curves. This time we only found two groups. Comparing them to the classifications above, they fall into two categories: four 'Unstable' and two 'Unfolded'. We show the mean curves for each group in Fig. 2b. The 'Unstable' simulations in this case fluctuate between 2 and 5 Å CαRMS from their starting structure. Likewise, the 'Unfolded' simulations demonstrate higher CαRMS values up past 8 Å. We will once more use these groupings to separate our discussion of these simulations.

2.6. Unstable

On average, the four simulations exhibiting 'Unstable' E42–E56 β-hairpin behavior bury on average 234 $Å^2$ of non-polar surface area and form on average five hydrogen bonds and one salt bridge. As was pointed out above, the CαRMS is a crude method for categorizing simulations. The ensemble of structures and/or pathways that can be sampled becomes larger the further a structure moves from its starting point [40]. This is the case with this grouping of runs, in that the four seem different from each other based on their individual interactions. However, looking at the averages of proteins interactions (Table 1B), we find that these simulations fall into two basic groups, which we name the 'A' and 'B' subgroups.

The E42–E56 'Unstable A' group consists of only one simulation. It buries more surface area (272 $Å^2$) than the other three due mainly to the

contributions from side-chain hydrophobic burial, but exhibits less hydrogen bonding and almost no salt bridges. Of the four 'Unstable' simulations, this one possesses the lowest CαRMS (data not shown). Looking at Table 2, we find that this simulation has many high occupancy intrastrand hydrophobic interactions with two at 100% occupancy. The hydrophobic core is centered on interactions from Y45 to D47, K50 and F52. The high occupancy of intrastrand, neighboring interactions (94% W43..Y45 and 90% T53..T55) and the low occupancy of interstrand hydrophobic interactions towards the termini (16% W43..V54) suggests that the β-hairpin's end is frayed. Only 4 hydrogen bonds are made on average, and these are also centered on the Y45 hydrophobic core. These hydrogen bonds are the native, main-chain hydrogen bonds in the plane of β-hairpin D46_H..T51_O and between side-chains Y45_HH..D47_OD. D46_OD does not make interactions with the peptide in this run. Somewhat surprising is the complete lack of salt bridges. Of course, the termini have denatured. Additionally, no salt bridge across the β-hairpin turn in conjunction with the lack of D46 side-chain interactions indicates the β-hairpin turn is largely unstructured.

The E42–E56 'Unstable B' group consists of three simulations. As shown in Table 1B, these bury 222 Å^2 of non-polar surface area on average. As can be seen by the occupancies in Table 2, this burial mainly comes from neighbors on the same side and strand of the β-hairpin: i to $i+2$ interactions like W43..Y45 at 73% and T49..T51 at 80%. These intrastrand hydrophobic contacts are loosely tied together by interactions that break the β-hairpin structure. Such interactions are not seen significantly in any of the other simulations, so they are not shown in Table 2. Their existence indicates that the β-hairpin structure has unfolded. Also, these unconventional hydrophobic contacts are not consistent between each of the three simulations in this group. In order to simplify the discussion of examples, we will number each simulation in this group as 'B1', 'B2' and 'B3'. The 'Unstable B1' simulation forms an interaction between Y45..T53 at 56% with 7 Å^2 burial, which is not seen in any other simulation above 7%. The 'Unstable B2' simulation makes contacts between T44..V54 at 70% with 8 Å^2 burial and D46..F52 at 97% with 9 Å^2 burial. These interactions are not seen above 1% in any other simulation under 'Stable' or 'Unstable' groupings, but they are seen at 30% in two 'Unfolded' simulations (one from each hairpin simulated). The 'Unstable B3' simulation exhibits a repacked hydrophobic core. As depicted in the top of Fig. 3, the hydrophobic core packs diagonally from the N-terminal strand to the C-terminal in the native β-hairpin. The 'Unstable B3' simulations possess the interaction from Y45..V54 at 83% with 12 Å^2 burial. This is not seen in any of the G41–E56 simulations and in only one other 'Unfolded' E42–E56 simulation at 15%. In addition, we find the T51..V54 contact at 50% with 5 Å^2 burial. Besides the Y45..V54 'Unstable B3' contact, all of these contacts are between residues that start on opposite sides of the β-hairpin (see Fig. 3), and therefore must break β-hairpin structure to form. The hydrogen bonding by D46 mostly contributes to the 6 average hydrogen bonds. The main salt bridge interaction D47_OD..K50_NZ occurs at the turn and persists 100% of the time in all 3 simulation.

2.7. Unfolded

On average, the two simulations exhibiting 'Unfolded' E42–E56 β-hairpin behavior are quite similar to their counterparts in the G41–E56 simulations. They bury 13 Å^2 more non-polar surface area at 226 Å^2. Even so, these simulations show high occupancies only in intrastrand, neighbor interactions between i to $i+2$ residues. The average number of hydrogen bonds is 8 and is primarily due to the hydrogen bond network formed by D46_OD. While on average two salt bridges are made, the only consistent one D47_OD..K50_NZ involves the β-hairpin turn. The other is split between E42_NT..E42_OE (a salt bridge within residue 42 shown as interaction 'l' on the hydrophilic side in Table 2) and K50_NZ..E56_OE (data not shown, since it only occurred in these simulations). Again, the image of these simulations is an opened β-hairpin that retains only its turn structure.

3. Discussion

Like previous theoretical work on the C-terminal, β-hairpin of protein G's B1 domain [31–37], our results are in good qualitative agreement with experiment [14,15,17] and find that the hydrophobic core made by residues W43, Y45, D47, K50, F52 and V54 are more important to stability than the main-chain hydrogen bonds. The importance of the turn to β-hairpin folding and stability has also been observed both experimentally [17,41,42] and in simulations studies [31,32,35,36,38]. However, a number of theoretical studies point out the importance of the hydrophobic core in the formation and stability of the β-hairpin [33,34,36]. By discussing our results in terms of the three protein interactions studied, we hope to provide clearer evidence for the importance of the turn in β-hairpin stability and folding; a picture of hydrophobic stabilization of the β-hairpin; and a role for salt bridge contribution to the stability of the β-hairpin.

3.1. Hydrogen bonds

As was shown explicitly by Ma and Nussinov in an elegant simulation study of the G41–E56 β-hairpin's [35], we find that the 9 native hydrogen bonds are unstable in all but one set of simulations (G41–E56's 'Stable A'). The most stable occur between the main-chain D46–T51 hydrogen bonding groups, and as the results of Dinner et al. suggest [34], these are not stable without the formation of the Y45–F52 hydrophobic interaction (compare the G41–E56's 'Stable' and 'Unstable' in Table 2). The work of Zhou et al. support this type of coupled hydrogen bond and hydrophobic interaction [30]. Other non-native hydrogen bonds can play more important roles in stabilizing the β-hairpin's fold. One such interaction is the D47_OD..Y45_HH, which helps to link the hydrophobic core to the turn. Absence of this hydrogen bond indicates that the β-hairpin is unfolded or has a rearranged structure (E42–E56 'Unstable B' group). Otherwise, in the G41–E56 'Stable' simulations, a constant number of hydrogen bonds are made from pool of candidates.

The most important hydrogen bonds in the β-hairpin are those made by the side-chain carboxyl of D46 and side-chain hydroxyl of T49. The stability of this hairpin has been found in a denaturation study of the full domain [42] as well as a simulation study of Protein G [38]. Even more conclusive are the NMR stability studies [15] and the Φ value analysis [41]. They provide strong support for the role of both side-chain's groups in stability of the β-hairpin and folding of the domain. We find interactions between these groups at high occupancy during stable simulations and are the major hydrogen bonds on the hydrophilic side of the β-hairpin. Without them, the β-hairpin's turn is largely destabilized as in the G41–E56 'Stable C' group and E42–E56 'Unstable A' simulation. Even more interesting, we find increased occupancies during both sets of unfolded trajectories. T49's contribution to stability is primarily limited to hydrogen bonds with D46, which may explain its lower contribution to the transition state in the Φ value analysis [41]. D46 makes a number of non-native hydrogen bonds across the turn as shown by Table 2 and the bottom of Fig. 3. This number allows D46 conformational flexibility to make hydrogen bonds and thus further contributes to stability. In folding, these numerous hydrogen bonds most likely help guide correct turn formation in the β-hairpin. Such an important network of hydrogen bonds has also been found in other systems [43].

3.2. Buried hydrophobic surface area

As expected, the G41-E56 'Stable' state exhibits hydrophobic core interactions between Y45..F52, F52..W43 and W42..V54 (see Fig. 3 and Table 2) predicted by experiment [14,15,17] and simulation [31–37]. This hydrophobic core repacks in the simulations, as was noted by Roccotano et al. [32], and increases the burial from the native by approximately 90 $Å^2$. On the hydrophilic side of the β-hairpin, the non-polar surface area is largely lost, especially towards the middle of the β-hairpin where there is a complete lack of interactions (see Fig. 3). For the contribution to the stability of the hydrophobic core, we need to compare between the G41–E56 'Stable A' simulations and the G41–E56 'Unfolded' simulations. Subtracting the difference between the total buried hydrophobic

surface areas gives a value of 74 Å^2. Using a previously calibrated conversion factor of 45 cal/mol·A^2 [44], we get approximately 3 kcal/mol of stabilization from the formation of the hydrophobic core. While this value seems small, this β-hairpin is not very stable and has been found to be only 50% folded at room temperature [14]. We do see alternative packing for the hydrophobic core in the G41–E56 'Stable C' simulations. Also, possible collapsed intermediates may be represented by the E42–E56 'Unstable B' simulations.

3.3. Salt bridges

The β-hairpin fold has stabilizing salt bridges at two places in the structure, as shown in Fig. 3. The side-chain groups of K50 and D47 form a salt bridge just before the turn, and the amino terminal group of G41 makes a salt bridge to either of the two-carboxyl groups of E56, which holds the free ends of the hairpin together. Intrastrand salt bridges, such as those between the free N-terminal group to the side-chain carboxyl of E42 and K50's amino to either of E56's carboxyls, do not contribute to β-hairpin stability as they can also be formed in the unfolded state.

As shown in Table 2, the salt bridge of D47_OD..K50_NZ is present with high occupancy in almost all simulations and would seem to contribute to the stability of the β-hairpin, especially at the turn. Experimental work making the mutation K50A shows it to be destabilizing for the β-hairpin [15]. These NMR stability experiments rank the K50A as less destabilizing than the D46A, but more than the T49A. These simulations help confirm the role of the D47 carboxyl to K50 amino salt bridge contribution to the stability of the turn and to the overall β-hairpin.

At the open end of the β-hairpin, the role of the stabilizing salt bridges is also clear but less obvious. Here the β-hairpin has a choice of the free N-terminal amino to either of E56's carboxyl groups. Of the G41–E56 'Stable' simulations, the 'A' group doesn't really make the salt-bridge, although in both 'B' and 'C' β-hairpin simulations one of the two salt bridges between the termini is made. In the G41–E56 'Unstable' simulations, we find that only the salt bridge at the termini keeps the β-hairpin from opening up, since the hydrophobic core has fallen apart. Complete lack of salt bridge occupancy is only seen in the G41–E56 'Unfolded' group. To test the idea of the terminal salt bridge contribution to stability, we ran six more simulations of a shorter peptide E42–E56. With the charged N-terminal one residue out of register, the salt bridge between the chain termini are not made with any consistency. As a result, the simulations are all less stable or unfolded. The E42–E56 'Unstable' simulations all allow for the rearrangement of the hydrophobic core. For the E42–E56 'Unstable A', this has a stabilizing consequence, but for the other three in the E42–E56 'Unstable B' group, the rearrangement allows for interactions that break β-hairpin structure. The E42–E56 'Unfolded' group is much like the G41–E56 one. To get at a value for the contribution of a salt bridge across the termini, we compare the G41–E56 'Stable A' to the G41–E56 'Stable B' simulations. In the 'Stable A' simulations, there is more hydrophobic burial and a decreased frequency of the terminal salt bridges. In the 'Stable B' simulations, the N-terminal amino to C-terminal carboxyl is always made, but there is less buried non-polar surface area. If we use this decrease in hydrophobic burial as a measure, we get that the salt bridge is equivalent to approximately 29 Å^2 of buried hydrophobic surface area or 1.3 kcal/mol using the aforementioned conversion factor [44]. Experimental support for terminal stabilization was done when a mutant peptide of the G41–E56 β-hairpin that possessed a disulfide across the termini was shown to be more stable [21]. A recent simulation study of another β-hairpin from Tendamistat that already possesses a disulfide at its termini also showed the increased stability of a closed β-hairpin [45].

4. Conclusion

The molecular dynamics simulations performed in this study support a folding scenario that matches more with the 'zipper' model [17], but is not mutually exclusive of the hydrophobic collapse model. Previous work [30] has suggested a compromise between the hydrogen bond centric view of the 'zipper model' and the hydrophobic centric view of the collapse model. We also prefer a

hybrid model; however, ours includes the hairpin and suggests that the hydrophobic residues act as the 'zipper' to help bring the hydrogen bonds in line. This takes into consideration the evidence that the hydrophobic core contributes to the bulk of the stability [29–37], but also includes the importance of the hydrogen bond interactions, which have also been shown to contribute to β-hairpin stability [30,34–36]. One major difference in this study to previous ones is that we did not use an acetylated and/or *N*-methylated peptide. This allowed for the ends to salt bridge and we found that salt bridges do contribute to the stability by trading off with hydrophobic burial and hydrogen bonds.

Because the G41–E52 β-hairpin folds on the order of microseconds in solution [17] and our simulations are only in the nanosecond regime, we cannot say that we have sampled all states of the equilibrium ensemble. We do believe we have sampled enough of the folded ensemble space to provide a good picture of the stability and insights into the folding of the G41–E52 β-hairpin, especially since our results corroborate what is seen experimentally [13–21]. We were somewhat concerned with our finding that only 7 of 12 simulations exhibited stable behavior (Table 1). Previous theoretical work found greater stability of the hairpin, although they were primarily probing for folding pathways [29–37]. Experimentally, Honda, et al. [14] found that 50% of the G41–E52 peptide is folded at room temperature. Even with 5 out of 12 simulations exhibiting unstable or unfolded behavior (see Table 1), our results of 58% are quite close to the stability found experimentally. Additionally, our findings about the stabilization of the turn by D46 and T49 hydrogen bonds as well as the salt bridge between D47 and K50 indicate that the β-hairpin's turn forms first, which supports experimental [15,41,42] and theoretical [38] findings about this turn. Then the non-polar residues collapse into a hydrophobic core. Salt bridges between the terminal residues help stabilize this core by closing the termini and preventing the core from opening up again. The hydrogen bonds are made last. This order makes sense in view of our simulations. The only time we find a hydrophobic core with an unstable turn is in 'Stable' simulations and the 'Unstable A' simulation. In the remaining more disordered states, where the hydrophobic core is less well packed, we always find strong hydrogen bonding and salt bridging interactions across turn. Hydrogen bonding along the main-chain is weak in most all of the simulations. This folding pathway also makes more logical sense. If the hydrophobic core were to form first, how would it know to bend the turn in the correct direction, since it is a non-specific force? Hydrophobic collapse into a left-handed turn would require substantial rearrangements to form the proper right-handed turn. Therefore, we argue that the local structure around the turn determines that the bend is right handed, but it is the hydrophobic collapse into a core that provides the stabilization necessary for the formation of the remainder of the β-hairpin. Salt bridges do contribute to this stabilization of the folding, but are not the driving forces behind it.

5. Methods

All simulations used the ENCAD program and potentials [39] They were set up and run with the same minimization steps as in the previous study [46]. The hairpin (residues G41–E56) edited out from the PDB file of the 1pgb structure [47] was placed in a box of waters. The box was then trimmed so that the edge of the box was at least 8 Å from the closest peptide atom. All waters within 1.67 Å of a hairpin atom were removed. The box sides were then correctly scaled to match the density of water (0.997 g/ml at 298 K). For the G41–E56 hairpin, there were 1055 waters in box with sides of 28.42 Å by 43.68 Å by 27.368 Å. For the E42–E56, there were 1039 waters in a box of 28.29 Å by 43.48 Å by 27.24 Å. This rectangular box has some limitations for a completely unfolding of the peptide. The box has the potential to interact with itself. This poses a problem; however, the trajectories seen here did not unfold to the extent that the peptide came within the non-bonded cutoff of 8 Å of itself. To completely accommodate the unfolded 16 mer, we would need to have square box with approximately 72 Å sides. Computationally, the numbers of waters would be prohibitive, even if the square box were truncated to some regular polyhedron.

Beginning from the native state and sampling conformations around it, the choice of the smaller water box for computational efficiency seemed reasonable.

We used a 2 femtosecond time step and coordinates were output every picosecond (every 500 steps). The trajectory was run for 10 ns at temperature of 298 K. Simulations were all run on Intel Pentium machines with the Linux operating system. Different runs used a different seed number for the initial, random assignment of velocities during the temperature equilibration of the system. The trajectories were viewed using the program MOLMAN.

All analyses were done using original code, which was written in FORTRAN, C and PERL. The CαRMS was calculated using the method of Kabsch [48]. Hydrogen bonds were measured between hydrogens connected to oxygen or nitrogen and acceptor oxygens. For a hydrogen bond to be made, the distance between hydrogen and acceptor oxygen needed to be less than 2.8 Å and the angle formed by the acceptor oxygen, hydrogen, and its covalently donor atom had to be greater than 120°. Hydrophobic contacts were measured using Voronoi polyhedra as described in detail previously [49]. A contact consisted of two carbon atoms sharing a polyhedron face. Salt bridges were assigned using a simple distance cutoff of 3.5 Å between the positively charged nitrogen of the amino group and the negatively charged oxygen of the carboxyl group.

Acknowledgments

Jerry Tsai and Michael Levitt would like to thank Bill Eaton for helpful discussions with this work. They would also like to thank the NIH (GM41455) for support. An NSF Biological Informatics Fellowship also supported Jerry Tsai.

References

[1] L. Pauling, R.B. Corey, H.R. Branson, The structure of proteins: two hydrogen-bonded helical configurations of the polypeptide chain, Proc. Natl. Acad. Sci. USA 37 (1951) 205–211.

[2] L. Pauling, R.B. Corey, Configurations of polypeptide chains with favored orientations around single bonds: two new pleated sheets, Proc. Natl. Acad. Sci. USA 37 (1951) 729–740.

[3] K. Linderstrøm-Lang, J.A. Schellman, Protein structure and enzymatic activity, in: H. Lardy, K. Myrback (Eds.), The Enzymes, New York, Academic Press, 1959, pp. 443–510.

[4] J.A. Schellman, Temperature, stability, and the hydrophobic interaction, Biophys. J. 73 (6) (1997) 2960–2964.

[5] J.A. Schellman, N.C. Gassner, The enthalpy of transfer of unfolded proteins into solutions of urea and guanidinium chloride, Biophys. Chem. 59 (3) (1996) 259–275.

[6] B.L. Chen, J.A. Schellman, Low-temperature unfolding of a mutant of phage T4 lysozyme. 1. equilibrium studies, Biochemistry 28 (2) (1989) 685–691.

[7] J.A. Schellman, The thermodynamic stability of proteins, Annu. Rev. Biophys. Biophys. Chem. 16 (1987) 115–137.

[8] R. Hawkes, M.G. Grutter, J. Schellman, Thermodynamic stability and point mutations of bacteriophage T4 lysozyme, J. Mol. Biol. 175 (2) (1984) 195–212.

[9] A. Chakrabartty, T. Kortemme, R.L. Baldwin, Helix propensities of the amino acids measured in alanine-based peptides without helix-stabilizing side-chain interactions, Protein Sci. 3 (5) (1994) 843–852.

[10] H. Qian, J.A. Schellman, Helix–coil theories: a comparative study for finite length peptides, J. Phys. Chem. 96 (1992) 3987–3994.

[11] A.J. Doig, R.L. Baldwin, N- and c-capping preferences for all 20 amino acids in alpha–helical peptides, Protein Sci. 4 (7) (1995) 1325–1336.

[12] S.S. Sung, Helix folding simulations with various initial conformations, Biohpys. J. 66 (1994) 1796–1803.

[13] S.R. Griffiths-Jones, A.J. Maynard, M.S. Searle, Dissecting the stability of a beta-hairpin peptide that folds in water: NMR and molecular dynamics analysis of the beta-turn and beta-strand contributions to folding, J. Mol. Biol. 292 (5) (1999) 1051–1069.

[14] S. Honda, N. Kobayashi, E. Munekata, Thermodynamics of a beta–hairpin structure: evidence for cooperative formation of folding nucleus, J. Mol. Biol. 295 (2) (2000) 269–278.

[15] N. Kobayashi, et al., Role of side-chains in the cooperative beta-hairpin folding of the short C-terminal fragment derived from streptococcal protein, G. Biochem. 39 (21) (2000) 6564–6571.

[16] T. Kortemme, M. Ramirez-Alvarado, L. Serrano, Design of a 20-amino acid, three-stranded beta-sheet protein, Science 281 (5374) (1998) 253–256.

[17] V. Muñoz, et al., Folding dynamics and mechanism of beta-hairpin formation, Nature (London) 390 (6656) (1997) 196–199.

[18] M. Ramirez-Alvarado, et al., Beta-hairpin and beta-sheet formation in designed linear peptides, Bioorg. Med. Chem. 7 (1) (1999) 93–103.

[19] F.J. Blanco, G. Rivas, L. Serrano, A short linear peptide that folds into a native stable beta-hairpin in aqueous solution, Nat. Struct. Biol. 1 (9) (1994) 584–590.
[20] N., Kobayashi, S. Endo, E. Munekata, Conformational study on the IgG binding domain of protein G. Peptide Chem. 1992, 1993: p. 278–280.
[21] N. Kobayashi, S. Honda, E. Munekata, Fragment reconstitution of a small protein: disulfide mutant of a short C-terminal fragment derived from streptococcal protein G, Biochemistry 38 (11) (1999) 3228–3234.
[22] K. Constantine, M. Friedrichs, T. Stouch, Extensive molecular dynamics simulations of β-hairpin forming peptide, Biopolymers 39 (1996) 591–614.
[23] M. Prevost, I. Ortmans, Refolding simulations of an isolated fragment of barnase into a native-like beta hairpin: evidence for compactness and hydrogen bonding as concurrent stabilizing factors, Proteins 29 (2) (1997) 212–227.
[24] L. Pugliese, M. Prevost, S.J. Wodak, Unfolding simulations of the 85–102 beta-hairpin of barnase, J. Mol. Biol. 251 (3) (1995) 432–447.
[25] D.J. Tobias, S.F. Sneddon, C.L. Brooks, Stability of a model beta-sheet in water, J. Mol. Biol. 227 (4) (1992) 1244–1252.
[26] F.B. Sheinerman, C.L.I. Brooks, A molecular dynamics simulation study of segment b1 of protein g, Proteins Struct. Funct. Gen. 29 (2) (1997) 193–202.
[27] A.S. Yang, B. Honig, Free energy determinants of secondary structure formation: II. Antiparallel beta-sheets, J. Mol. Biol. 252 (3) (1995) 366–376.
[28] A. Li, V. Daggett, Molecular dynamics simulation of the unfolding of barnase: characterization of the major intermediate, J. Mol. Biol. 275 (4) (1998) 677–694.
[29] A.E. Garcia, K.Y. Sanbonmatsu, Exploring the energy landscape of a beta hairpin in explicit solvent, Proteins 42 (3) (2001) 345–354.
[30] R. Zhou, B.J. Berne, R. Germain, The free energy landscape for beta hairpin folding in explicit water, Proc. Natl. Acad. Sci. USA 98 (26) (2001) 14931–14936.
[31] A. Kolinski, B. Ilkowski, J. Skolnick, Dynamics and thermodynamics of beta-hairpin assembly: insights from various simulation techniques, Biophys. J. 77 (6) (1999) 2942–2952.
[32] D. Roccatano, et al., A molecular dynamics study of the 41–56 beta-hairpin from B1 domain of protein G, Protein Sci. 8 (10) (1999) 2130–2143.
[33] V.S. Pande, D.S. Rokhsar, Molecular dynamics simulations of unfolding and refolding of a beta- hairpin fragment of protein G, Proc. Natl. Acad. Sci. USA 96 (16) (1999) 9062–9067.
[34] A.R. Dinner, T. Lazaridis, M. Karplus, Understanding beta-hairpin formation, Proc. Natl. Acad. Sci. USA 96 (16) (1999) 9068–9073.
[35] B. Ma, R. Nussinov, Molecular dynamics simulations of a beta-hairpin fragment of protein G: balance between side-chain and backbone forces, J. Mol. Biol. 296 (4) (2000) 1091–1104.
[36] B. Zagrovic, E.J. Sorin, V. Pande, beta-hairpin folding simulations in atomistic detail using an implicit solvent model, J. Mol. Biol. 313 (1) (2001) 151–169.
[37] J. Lee, S. Shin, Understanding beta-hairpin formation by molecular dynamics simulations of unfolding, Biophys. J. 5 (2001) 2507–2516.
[38] F.B. Sheinerman, C.L. Brooks, Calculations on folding of segment B1 of streptococcal protein G, J. Mol. Biol. 278 (2) (1998) 439–456.
[39] M. Levitt, et al., Potential energy function and parameters for simulation of the molecular dynamics of proteins and nucleic acids in solution, Comp. Phy. Comm. 91 (1995) 215–231.
[40] J.D. Bryngelson, et al., Funnels, pathways, and the energy landscape of protein folding: a synthesis, Proteins 21 (3) (1995) 167–195.
[41] E.L. McCallister, E. Alm, D. Baker, Critical role of beta-hairpin formation in protein G folding, Nat. Struct. Biol. 7 (8) (2000) 669–673.
[42] M.K. Frank, G.M. Clore, A.M. Gronenborn, Structural and dynamic characterization of the urea denatured state of the immunoglobulin binding domain of streptococcal protein G by multidimensional heteronuclear NMR spectroscopy, Protein Sci. 4 (12) (1995) 2605–2615.
[43] V.P. Grantcharova, et al., Important role of hydrogen bonds in the structurally polarized transition state for folding of the src SH3 domain, Nat. Struct. Biol. 5 (8) (1998) 714–720.
[44] T.M. Raschke, J. Tsai, M. Levitt, Quantification of the hydrophobic interaction by simulations of the aggregation of small hydrophobic solutes in water, Proc. Natl. Acad. Sci. USA 98 (11) (2001) 5965–5969.
[45] A.M. Bonvin, W.F. van Gunsteren, Beta-hairpin stability and folding: molecular dynamics studies of the first beta-hairpin of tendamistat, J. Mol. Biol. 296 (1) (2000) 255–268.
[46] M. Levitt, Molecular dynamics of native protein. I. Computer simulation of trajectories, J. Mol. Biol. 168 (1983) 595–620.
[47] T. Gallagher, et al., Two crystal structures of the b1 immunoglobulin-binding domain of streptococcal protein g and comparison with nmr, Biochemistry 33 (15) (1994) 4721–4729.
[48] W. Kabsch, A discussion of the solution for the best rotation to relate two sets of vectors, Acta Crystall. A34 (1978) 827–828.
[49] M. Gerstein, J. Tsai, J. Levitt, The volume of atoms on the protein surface: calculated from simulation, using *voronoi polyhedra*, J. Mol. Biol. 249 (1995) 955–966.
[50] R. Sayle, E.J. Milner-White, RasMol: Biomolecular graphics for all, TIBS 20 (9) (1995) 374.
[51] P.J. Kraulis, MOLSCRIPT: A program to produce both detailed and schematic plots of protein structures, J. App. Cryst. 24 (1991) 946–950.